2018

Whispering Gallery Mode Micro Resonators for Multi-Parameter Applications

Arun Mallik
Technological University Dublin, arun.mallik@tudublin.ie

Gerald Farrell
Technological University Dublin, gerald.farrell@tudublin.ie

Manjusha Ramakrishnan
Technological University of Dublin, manjusha.ramakrishnan@mydit.ie

See next page for additional authors

Recommended Citation

Mallik, K., Farrell, G. & Ramakrishnan, M. (2018). Whispering gallery mode micro resonators for multi-parameter applications. *Optics Express*, vol. 26, no. 24, pg. 31829-31838. doi:10.1364/OE.26.031829

Research Article | Vol. 26, No. 24 | 26 Nov 2018 | OPTICS EXPRESS 31829
Optics EXPRESS

Whispering gallery mode micro resonators for multi-parameter sensing applications

ARUN KUMAR MALLIK,[1,*] GERALD FARRELL,[1] MANJUSHA RAMAKRISHNAN,[1] VISHNU KAVUNGAL,[1] DEJUN LIU,[1] QIANG WU,[2] AND YULIYA SEMENOVA[1]

[1]*Photonics Research Centre, Dublin Institute of Technology, Kevin Street, Dublin 8, Ireland*
[2]*Department of Mathematics, Physics and Electrical Engineering, Northumbria University, Newcastle Upon Tyne, NE1 8ST, United Kingdom*
[*]*arun.kumarmallik@mydit.ie*

Abstract: A novel fiber optic sensing configuration for simultaneously measuring ammonia vapor (NH_3) concentration and relative humidity (RH) in air is proposed and experimentally demonstrated. The system comprised two silica whispering gallery mode (WGM) microsphere resonators coated with different polymer layers. One of the microspheres was dip-coated with sol gel silica polymer and another with a 0.5 % wt./vol. agarose hydrogel. WGMs in both microspheres were excited simultaneously by evanescent coupling using a single adiabatic fiber taper. The optical properties of both coating layers change due to their exposure to ammonia and water molecules in the surrounding atmosphere, resulting in the spectral shifts of the WGM resonances relevant to each of the microspheres. By measuring the relevant WGMs' spectral shifts, the NH_3 concentration in air and the RH can be determined simultaneously. The experimentally demonstrated sensitivity of the proposed sensor array to ammonia was estimated as 19.07 pm/ppm (NH_3 molecules in air) and its sensitivity to relative humidity as 1.07 pm/% RH. Detailed studies of the coatings' cross-sensitivity and temperature dependence are also presented. The proposed sensor array is compact, highly sensitive and potentially low cost.

1. Introduction

Whispering gallery mode (WGM) microsphere resonators have been successfully investigated as sensors in numerous areas including refractive index, temperature, force, electromagnetic field, gas, and bio sensing in recent years due to their high quality factors (Q), low mode volume and inexpensive fabrication processes [1–7]. The WGM operating principle relies on strong confinement of light through total internal reflection inside the microcavity and retaining the same phase after each cycle of propagation. Silica microspheres are shaped by natural surface tension forces during fabrication, resulting in a clean, smooth silica surface with very minimal loss and negligible scattering, making such silica microspheres suitable for the next generation of high-performance optical sensors. The spectral positions of WGM resonances are strongly dependent on the geometry of the dielectric resonator (diameter, sphericity), the optical properties of the resonator material and also on the refractive index (RI) of the medium in the environment surrounding the resonator. Either a very small deformation of the microcavity or a minute change in material properties (such as RI) can be easily quantified by monitoring the WGM resonance wavelength shift. Much of the research effort to date has been focused on using a single WGM resonator to sense a single physical, chemical or biological quantity, with only limited research focused on multi-parametric sensing [8]. However, in real life applications simultaneous sensing of multiple parameters is often required. Many effective techniques have been developed to realize multi-parametric measurements with fiber optic sensors. For example, simultaneous measurement of humidity and temperature has been proposed using a combination of a long period grating (LPG) inscribed in a fiber loop mirror [9], a combination of a fiber Bragg grating (FBG)

#335005 https://doi.org/10.1364/OE.26.031829
Journal © 2018 Received 13 Jun 2018; revised 17 Aug 2018; accepted 18 Aug 2018; published 19 Nov 2018

Optics EXPRESS

and Fabry-Perot interferometer cavity [10], a FBG and photonics crystal fiber interferometer [11], a LPG partially coated with PAH/PAA poly electrolyte complexes [12], nafion-crystal violet film based optical sensor is to measurement of humidity and ammonia in air simultaneously [13], nano porous layer of alumina is also proposed for sensing of both humidity and ammonia gas [14] and many others. All the above mentioned sensing techniques rely on measurements of characteristic wavelength shifts in the spectra of the sensors influenced by the physical parameters of interest. Some of these configurations suffer from complexity of interrogation and a poor wavelength resolution. WGM microsphere resonators have advantage over the sensors above due to their high Q-factors (up to 10^9) [15], resulting in much higher wavelength resolution and low detection limits. Recently we proposed and demonstrated an highly sensitive relative humidity (RH) sensor based on a silica microsphere coated with a thin layer of agarose hydrogel [16]. We have also demonstrated a silica gel coated silica microsphere for a very low detection limit ammonia sensing and a silica gel coated optical fiber sensors for highly sensitive detection of ammonia in water [17, 18].Ammonia is a colorless, highly corrosive and toxic gas with pungent smell which has adverse effects on human health including burning nose, throat and respiratory track irritation even after a long term exposure at lower concentrations of ammonia [19, 20]. Therefore, some means to sense and also quantify ammonia concentration in air is needed. Similarly, humidity is one of the important environmental conditions which plays a very significant role in agriculture, the food industry, clinical medicine, manufacturing, civil engineering, textile manufacture, the semiconductor industry and many other fields. Humidity measurement in industries is critical because it may affect the quality of the product, for example the shelf-life of foodstuffs. Hence, humidity sensing is very important, especially in the control systems for industrial processes. In many of the applications listed above, a means for simultaneous measurement of ammonia concentration in air and RH is required. For example, a recent study by Wei et al. demonstrated a strong influence of both NH_3 concentration and ambient RH on the immune system of broiler chickens, highlighting the need for simultaneous monitoring and control of both parameters in the atmosphere of poultry or animal houses [21].

In this article, we propose a novel fiber optic sensor's configuration for simultaneous measurement of both ammonia concentration and relative humidity in air. To realize this we excited WGMs in two microspheres coupled to the same optical fiber taper. The two microspheres have nearly the same diameter of 250 μm and 255 μm and were used to measure ammonia and humidity simultaneously. An adiabatic tapered fiber with the uniform waist diameter of 3-4 μm was used to simultaneously couple the light into both microspheres forming a small array. One of the microspheres was coated with a layer of sol-gel silica whose optical properties are very sensitive to ammonia, while the second microsphere was coated with a highly hygroscopic layer of 0.5 % wt./vol. agarose hydrogel. To the best of our knowledge this study is the first experimental demonstration of multi-parametric sensor based on the WGM phenomenon that offers simultaneous high resolution measurement of both ammonia concentration in air and relative humidity. A study of the temperature sensitivity of the proposed sensing system was also performed showing minimal temperature dependence compared to other fiber optic sensors.

2. Sensor Fabrication and Experimental setup

In our experiment the agarose hydrogel for the coating was made from a commercially available agarose powder from Sigma Aldrich (A6013). The hydrogel solution was prepared by adding 0.5% wt./vol. of the agarose powder mixed in deionized (DI) water, followed by continuous stirring at 80°C temperature until all the agarose powder was completely dissolved in the DI water. Preparation of the sol-gel silica coating was carried as described in ref. [22]. The sol-gel was prepared by hydrolysis and condensation of TEOS (Tetraethyl ortho silicate) in presence of water and ethanol. The molar ratio of TEOS, ethyl alcohol and DI water was 1:4:16 mixed in a 250-mL measuring flask and kept at continuous stirring conditions for 1.5 hour. 3-4 drops

Optics EXPRESS

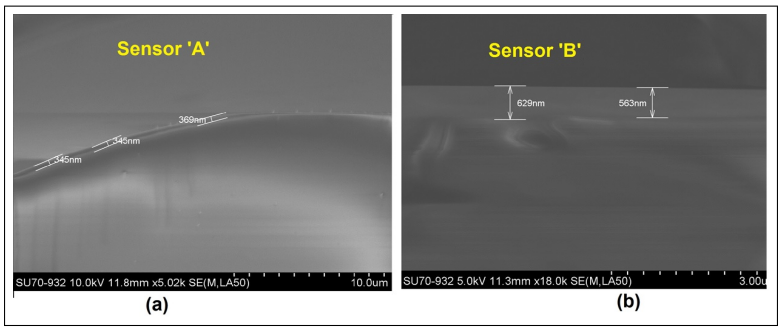

Fig. 1. SEM images of cross sections of singlemode fibers coated with (a) silica sol-gel; (b) 0.5% wt. vol. agarose hydrogel.

of hydrochloric acid (HCL) were used as catalyst. The solution was kept for two days at room temperature. Both silica microspheres were fabricated at the tip of an unjacketed cleaved single mode fiber using the electric arc of a fusion splicer, as described in [16]. After applying a series of 3 electric discharge arcs to the cleaved surface of the fiber tip using a fusion splicer, the fiber tip assumed spherical shape due to surface tension. Two microspheres of almost the same diameter (250 μm and 255 μm) were prepared for our experiments. Agarose and silica coating layers were applied separately on each of the microsphere's surfaces by dip coating method with the pulling speed of 2 mm/sec. For identification we labeled the silica gel coated microsphere as sensor 'A' and the agarose coated microsphere as sensor 'B'. Both microspheres were kept dry at room temperature for 24 hours before the experiments. The coating thickness was estimated by analyzing the SEM images of cross-sections of singlemode fiber ends dip coated with the respective gels using the same method and pulling speed (2 mm/sec), similarly dried and cleaved. Figure 1 shows the SEM images of the respective cleaved surfaces where the thickness of the coating is measured as 300 - 400 nm for the silica gel and 500-600 nm for agarose.

To allow for coupling of light in and out of the microspheres, an adiabatic tapered fiber was fabricated using a customized micro heater brushing technique [23]. In our experiment the tapered waist diameter was approximately 3-4 microns. To improve mechanical stability, the fabricated fiber taper was placed in direct contact with the microspheres and fixed on a glass slide at a height of 5 mm from the slide surface using two drops of UV curable epoxy (Norrland).A schematic diagram of the experimental setup is shown in Fig. 2. The experimental set up consisted of a broadband light source (Thorlabs S5FC1005S), polarization controller, optical spectrum analyzer (OSA, Advantest Q8384) and a temperature controlled humidity chamber (ETS 5503). Each coated microsphere was mounted on an XYZ nano-positioning stage and then slowly brought in contact with the tapered fiber inside the humidity chamber.

3. Results and Discussion

Light from the broadband superluminescent light source (SLD) operating in the wavelength range 1530-1570 nm was launched into the fiber taper and the corresponding transmission spectrum was observed at the taper output by means of the OSA. The wavelength resolution of the OSA was 10 pm. The WGM excitation in both microspheres was achieved by evanescent coupling to the tapered fiber. At first, the silica gel coated microsphere (sensor A) was gradually and carefully brought in direct contact with the tapered fiber until the WGM resonances were clearly observed in the transmission spectrum of the fiber taper. The input light polarization was adjusted using a manual polarization controller to achieve maximum light coupling efficiency. The transmission spectrum after coupling Sensor A is shown in Fig. 3, where WGM resonances near 1540.6 nm can be clearly seen. Without changing the setup, the second microsphere (sensor B) was

Optics EXPRESS

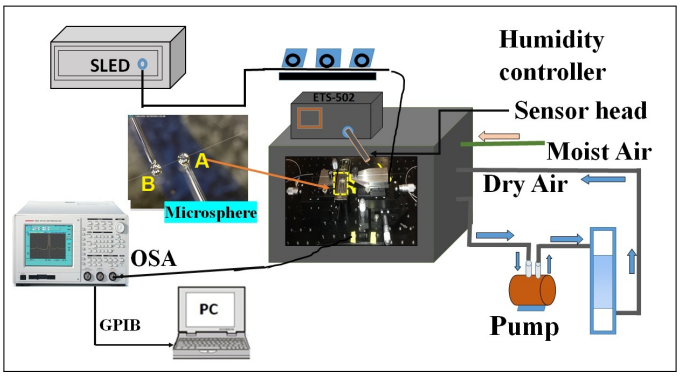

Fig. 2. Experimental setup for multi parameter sensor characterization.

positioned near the silica gel coated sphere and coupled to same tapered fiber. The resulting transmission spectrum showing the WGM resonances due to both microspheres is labelled "A+B" in Fig. 3. Red curve "Sensor B" in Fig. 3 illustrates the WGM spectrum of the tapered fiber when only sensor B is coupled. As one can see from the figure, both groups of "A" and "B" resonances are clearly visible and distinguishable in the combined "A+B" spectrum. The optical

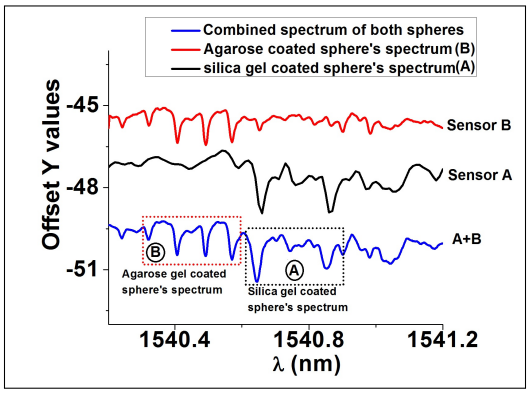

Fig. 3. Transmission WGM spectra for both sensors separately and when both microspheres are coupled simultaneously.

properties of the agarose coating are very sensitive to relative humidity, while those of the silica coating strongly depend on the ammonia concentration in the surrounding atmosphere and to a lesser extent on its relative humidity. Therefore changes in either of the parameters will result in spectral shifts of the WGM resonances, which can be expressed as:

$$\begin{bmatrix} \Delta\lambda_A \\ \Delta\lambda_B \end{bmatrix} = \begin{bmatrix} K_{11} & K_{12} \\ K_{21} & K_{22} \end{bmatrix} \begin{bmatrix} \%RH \\ \%NH_3 \end{bmatrix} \tag{1}$$

where K_{11} and K_{12} are the linear coefficients representing sensitivity of sensor A to relative humidity and ammonia concentration respectively.similarly, K_{21} and K_{22} are the ammonia sensitivities of sensor B. After experimental calibration of the sensors and determining the values of the coefficients, it is possible to independently find both humidity and ammonia concentration.

Experimental measurements of humidity inside the humidity and temperature controlled

Optics EXPRESS

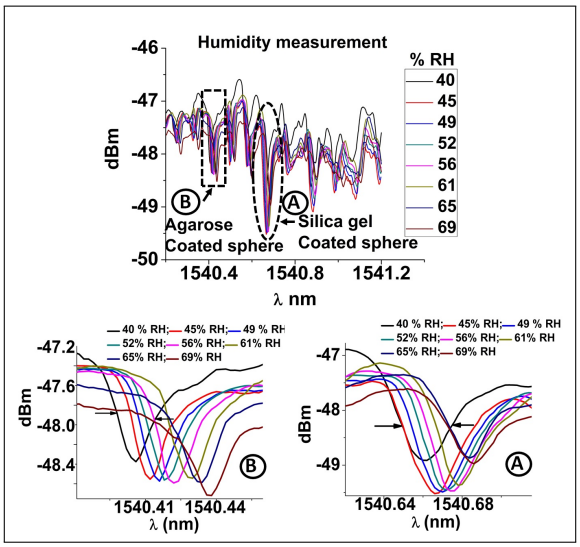

Fig. 4. Transmission spectrum for sensors A and B simultaneously at different humidity levels inside the chamber. The inset graphs are enlarged selected portions of the overall spectrum for sensors 'A' and 'B' at constant temperature of 25 ± 0.1 °C.

chamber were carried out with both sensors A and B in the range of relative humidity values from 40 % to 70 %RH at constant temperature of 25 ± 0.1 °C. The sensing mechanism for both sensors A and B are based on the change of effective refractive index and thickness of the coating layer due to adsorption of water vapor by the coating surface. This process leads to the air inside the micro pores of the coating layer being replaced with water molecules under capillary forces. As a result, the effective refractive index and thickness of the coating increases and WGMs experience a red spectral shift. Figure 4 represents the WGM spectra of both sensors at different levels of relative humidity in the chamber. A commercial electronic hygrometer was used as a reference for humidity measurement inside the chamber. The Q-factors of the selected WGMs for sensors A and B in Fig. 4 were estimated using equation Q= $\frac{\lambda_R}{\Delta\lambda_{FWHM}}$, where λ_R is the resonance wavelength and $\Delta\lambda_{FWHM}$ is the full width at half-maximum of the resonant lobe calculated by fitting the resonant dip with the Lorentzian function. The quality factors were calculated as Q =5.22×10^4 for sensor A and Q= 9.81×10^4 for sensor B, respectively

It should be noted the measured values of the Q-factor shown in Fig. 4 are lower compared to those reported in the literature for silica microspheres [2, 3]. One of the reasons is the limitations of the experimental setup employed in our experiment, which consisted of a broadband light source and optical spectrum analyzer with a wavelength resolution of 10 pm. Another reason might be the increased absorption and scattering loss due to the applied coatings on the surfaces of the microspheres. Figure 5 is a plot of the spectral shifts of the selected WGM resonances for sensors A and B as functions of relative humidity inside the chamber. One can see from the graph that both dependences are very close to linear and the corresponding sensitivities to humidity are K_{11}= 0.8 pm/%RH for sensor A and K_{21}=1.07 pm/%RH for sensor B. The same experimental setup was used to investigate the optical responses of the sensors A and B to different concentrations of ammonia vapors at constant temperature of 25 ± 0.1°C and constant humidity of 40% RH inside the chamber. A small amount of ammonium hydroxide (NH_4OH) liquid was injected into and then removed from the gas chamber after the measurement, in order to create three low ammonia vapor concentrations corresponding to 0.46 ppm, 1.46 ppm, and 2.19 ppm of ammonia in air. Spectral data were was recorded using an OSA connected to a PC

Optics EXPRESS

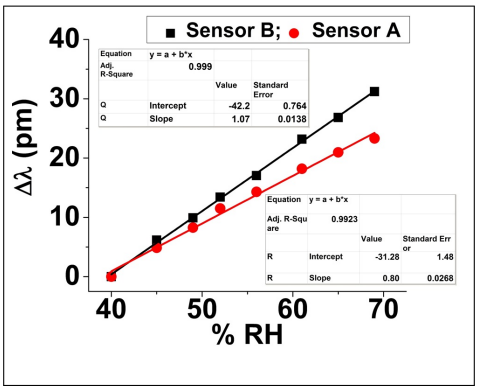

Fig. 5. Linear fitted graph of the selected WGM wavelengths versus relative humidity for both the silica gel coated (sensor A) and agarose coated (sensor B) microspheres.

through a GPIB cable and a customized LabView program. It should be noted that the WGM spectral shift dynamics depends on the diffusion rate of ammonia vapors inside the chamber.

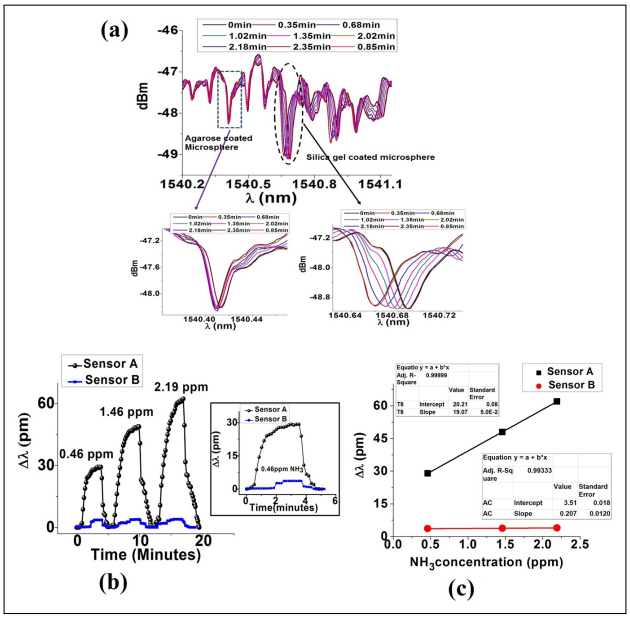

Fig. 6. (a) Transmission spectrum for the sensor system recorded at different times after injection of ammonia vapor in concentration of 0.46 ppm inside the chamber at constant temperature of 25 ± 0.1 °C and humidity 40% RH. Insets represent the enlarged portions of the spectrum corresponding to sensors A and B; (b) A and B WGM spectral shifts in response to three different concentrations of ammonia (0.46 ppm, 1.46 ppm and 2.19 ppm) after injection of the vapors inside the chamber. Inset figure illustrates the response to 0.46 ppm concentration of ammonia only; (c) WGM spectral shifts for the sensors A and B as a function of ammonia concentration.

Figure 6(a) illustrates the spectrum for both the microspheres coupled to the same tapered fiber after injection of ammonia vapor at 0.46 ppm concentration inside the chamber. As can be seen from the figure and inset A (dotted oval in the main graph), the WGM resonance associated with

Optics EXPRESS

the silica gel coated microsphere experiences red shift during the sensor's exposure to ammonia vapor. The corresponding spectral shift of the WGM resonance associated with sensor B (inset B, dotted rectangle in the main graph) also occurs in the direction towards the longer wavelengths but is much smaller. Figure 6(b) illustrates the dynamics of the WGM spectral shifts for both of the microspheres as they were exposed to 0.46 ppm, 1.46 ppm and 2.19 ppm concentrations of ammonia inside the chamber. The inset graph in Fig. 6(b) shows that the total shift of the selected WGM resonance wavelength for sensor A was approximately 95 times larger than that for the sensor B during their an exposure to 0.46 ppm ammonia vapor concentration. This is due to presence of silanol group on the surface of silica gel coated sphere producing ae dipole interaction between hydroxyl group and NH_3. The adsorption of these ammonia molecules on the surface of silica gel microsphere increases themuch higher sensitivity of the effective refractive index of silica gel coating more than to ammonia compared to that of the agarose layer on the surface of B microsphere. When the gas was removed from the chamber by opening its exhaust valve, the WGM resonances returned back to their original positions. Total spectral shifts of the WGM resonances for both the microspheres are plotted as a function of ammonia concentration in Fig. 6(c). The ammonia sensitivity coefficients K_{12} and K_{21} were derived from the linear fits of the experimental data as K_{12}=19.07 pm/ppm and K_{22}=0.2 pm/ppm at constant temperature of 25 ± 0.1 °C and 40% RH humidity.

It should be noted that the above sensitivity coefficients for both of the sensors were determined at a constant ammonia concentration (0.46ppm) and humidity (40%RH) level respectively, and at first were assumed to be independent. It is possible, however that both coatings have some cross-sensitivity issues, so that the values of the linear coefficients are not fully independent. In particular, the porous nature of the silica gel coating layer is more likely to make it susceptible to the presence of water molecules, affecting its sensitivity to ammonia at a different RH. To investigate this, we carried out an additional study of response of the silica gel coated microsphere towards ammonia at several different relative humidity levels, namely at 10, 22, 35, 45, 60 and 75% RH. Figure 7 shows the dependence of the sensor A sensitivity to ammonia (coefficient K_{12}) as a function of relative humidity at constant temperature of 25°C. The same values of ammonia concentrations as in the previous experiments were used in this study. As one can see from Fig. 7, sensitivity to ammonia for sensor A is a non-linear function of relative humidity in the chamber. Ammonia sensitivity decreases with an increase of relative humidity saturating above 60% RH. This is likely because ammonia molecules are more easily adsorbed by the surface water rather than the silica coating. Similarly, at lower humidity levels, a greater number of ammonia molecules are adsorbed directly on the surface of the silica coating pores resulting in greater change of the coating's effective refractive index due to ammonia.

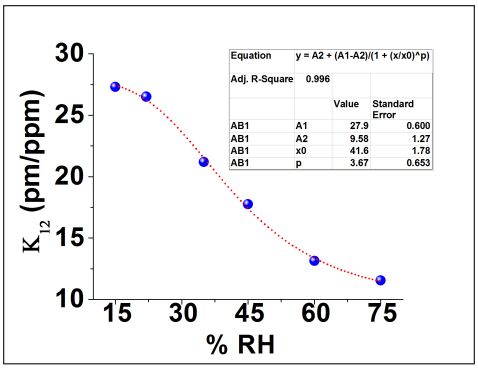

Fig. 7. K_{12} as a function of RH at constant temperature of 25°C

The fit of the experimental results with a logistic function in Fig. 7 gives the approximate

Optics EXPRESS

sensitivity of the sensor A in presence of humidity in the range from 15% RH to 75% RH with less than ±1% error.It is clear that K_{12} in Eq. (1) is not a constant independent of the humidity level. However the dependence of K_{12} on the humidity level is predictable and can be determined from the following approximate equation:

$$K_{12} = 9.58 + \frac{18.32}{1 + (\frac{\%RH}{41.6})^{3.67}} \tag{2}$$

Since K_{12} can no longer be considered as a constant, it appears that Eq. (1) can no longer be used for accurate detection of both parameters changing independently in the surrounding the sensor system atmosphere.

Substituting the K_{12} coefficient's values in Eq.(1) we get:

$$\begin{bmatrix} \Delta\lambda_A \\ \Delta\lambda_B \end{bmatrix} = \begin{bmatrix} K_{11} & 9.58 + \frac{18.32}{1+(\frac{\%RH}{41.6})^{3.67}} \\ K_{21} & K_{22} \end{bmatrix} \begin{bmatrix} \%RH \\ \%NH_3 \end{bmatrix} \tag{3}$$

To determine the value of K_{12} unambiguously one only needs to have an accurate value for the %RH level, which Sensor B can provide, and which is not dependent on the level of ammonia. Thus to determine the %RH and ammonia concentrations levels requires a two step approach. Assuming both sensors are calibrated, then as first step use Sensor B to measure %RH and then as a second step use the value of the %RH to determine the value of the coefficient K_{12} and then directly determine the ammonia concentration using this value and the measured wavelength shift for Sensor A.

A study of the influence of temperature on the performance of the proposed sensor array was also carried out using the same environmental chamber. The temperature inside the chamber was gradually increased in a step like fashion from 20 °C to 40 °C. Each WGM spectrum was recorded when the temperature inside the chamber was stable at the set point. Figure 8 shows the temperature responses of sensors A and B at 40 % RH. The linear fits of the experimental data allow to determine the temperature sensitivities as 5.8 pm/ °C for sensor A and 6.7 pm/°Cfor sensor B.

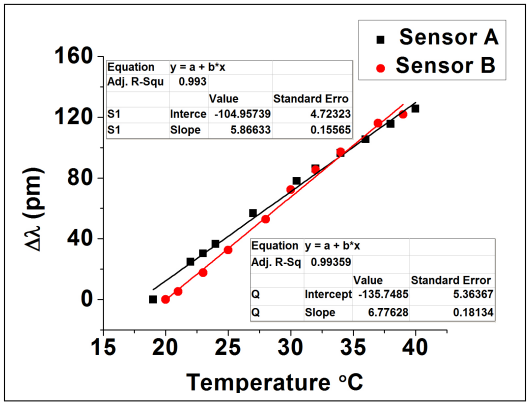

Fig. 8. Temperature dependence of the WGM spectral shift for sensors A and B at constant humidity of 40% RH.

The detection limit (DL) for a sensor represents the smallest measurable physical parameter change and it can be expressed as DL = $\frac{R}{S}$, where R is the resolution of the sensor and S is its

Optics EXPRESS

sensitivity. R can be calculated as

$$R = 3 \times \sqrt{\sigma_N^2 + \sigma_T^2 + \sigma_{SR}^2} \tag{4}$$

where σ_N, σ_T, σ_{SR} represent the standard deviations associated with the amplitude noise limited SNR of the detection system, temperature fluctuations and detector spectral resolutions respectively [24]. We assumed the signal-to-noise ratio of the system to be approximately 60 dB, so that $\sigma_N$is calculated as 0.2 pm and 0.1 pm for sensors A and B, respectively [24]. The standard deviation due to temperature stabilization is taken as σ_T = 0.01 pm for both the sensors. The error in determining the position of the resonant mode is uniformly distributed between -0.3 pm and +0.3 pm and the resulting standard deviation associated with the standard deviation of the spectral resolution of the broadband source is σ_{SR} = 0.17 [24] in both cases. The overall sensor resolution calculated for sensor A is R =0.8 pm and for sensor B is R =0.6 pm. The corresponding DLs for sensors A and B are listed in Table 1

Table 1. **Individual detection limit estimates for sensors A and B at 40 %RH**

Parameters	Humidity	Ammonia
Sensor A	1%RH	42 ppb
Sensor B	0.56%RH	3000 ppb

4. Conclusion

In conclusion, a novel approach to simultaneous measurement of ammonia vapor and humidity in air has been proposed and demonstrated experimentally. WGMs were excited at the same time in the array of two microspheres coated with different polymers, namely, silica gel and agarose hydrogel, coupled to a single adiabatic fiber taper. The experimental results revealed that the silica gel coated microsphere was more sensitive to ammonia than the agarose coated microsphere. Similarly, the agarose coated sphere had better sensitivity to humidity than the silica gel coated microsphere. It has been demonstrated that by monitoring the spectral positions of two WGM resonances relevant to each of the microspheres, it was possible to simultaneously determine ammonia concentration and relative humidity in the surrounding the array atmosphere. The maximum measurement resolutions of the two parameters were estimated as 42 ppb for ammonia and 5.6×10^{-1}%RH for humidity at the temperature of 25 ± 0.1°C. The proposed method offers the advantages interrogation using a single fibre along with a compact sensor size, high resolution and simple fabrication. The potential applications can be expanded to sensing of other chemical and biological quantities utilizing various coatings and possibly increasing the number of sensors within the array.

Funding

Enterprise Ireland and the European Regional Development Fund under Ireland's European Structural and Investment Funds Programme 2014-2020(CF-2016-0448-P); Qiang Wu acknowledges State Key Laboratory of Advanced Optical Communication Systems and Networks, Shanghai Jiao Tong University, China.

Acknowledgment

Arun Kumar Mallik acknowledges the support of the Dublin Institute of Technology and the Fiosraigh Dean of Graduate Students scholarship.

Optics EXPRESS

References

1. N. M. Hanumegowda, C. J. Stica, B. C. Patel, I. White, and X. Fan, "Refractometric sensors based on microsphere resonators," Appl. Phys. Lett. **87**, 1–3 (2005).
2. Q. Ma, T. Rossmann, and Z. Guo, "Whispering-gallery mode silica microsensors for cryogenic to room temperature measurement," Meas. Sci. Technol. **21**, 129501 (2010).
3. T. Ioppolo, M. Kozhevnikov, V. Stepaniuk, M. V. Ötügen, and V. Sheverev, "Micro-optical force sensor concept based on whispering gallery mode resonators," Appl. Opt. **47**, 3009–3014 (2008).
4. T. Ioppolo, U. Ayaz, and M. V. Otugen, "Tuning of whispering gallery modes of spherical resonators using an external electric field," Opt. Express **17**, 16465–16479 (2009).
5. V. Ilchenko, P. Volikov, V. Velichansky, F. Treussart, V. Lefèvre-Seguin, J.-M. Raimond, and S. Haroche, "Strain-tunable high-Q optical microsphere resonator," Opt. Commun. **145**, 86–90 (1998).
6. N. Lin, L. Jiang, S. Wang, Q. Chen, H. Xiao, Y. Lu, and H. Tsai, "Simulation and optimization of polymer-coated microsphere resonators in chemical vapor sensing," Appl. Opt. **50**, 5465 (2011).
7. F. Vollmer, D. Braun, A. Libchaber, M. Khoshsima, I. Teraoka, and S. Arnold, "Protein detection by optical shift of a resonant microcavity," Appl. Phys. Lett. **80**, 4057–4059 (2002).
8. F. Vollmer, S. Arnold, D. Braun, I. Teraoka, and A. Libchaber, "Multiplexed DNA quantification by spectroscopic shift of two microsphere cavities," Biophys. J. **85**, 1974–1979 (2003).
9. H. Liu, H. Liang, M. Sun, K. Ni, and Y. Jin, "Simultaneous measurement of humidity and temperature based on a long-period fiber grating inscribed in fiber loop mirror," IEEE Sensors J. **14**, 893–896 (2014).
10. F. J. Arregui, I. R. Matías, K. L. Cooper, and R. O. Claus, "Simultaneous measurement of humidity and temperature by combining a reflective intensity-based optical fiber sensor and a fiber bragg grating," IEEE Sensors J. **2**, 482–487 (2002).
11. J. Mathew, Y. Semenova, and G. Farrell, "Fiber optic hybrid device for simultaneous measurement of humidity and temperature," IEEE Sensors J. **13**, 1632–1636 (2013).
12. A. Urrutia, J. Goicoechea, A. L. Ricchiuti, D. Barrera, S. Sales, and F. J. Arregui, "Simultaneous measurement of humidity and temperature based on a partially coated optical fiber long period grating," Sens. Actuators B: Chem. **227**, 135–141 (2016).
13. I. M. Raimundo and R. Narayanaswamy, "Simultaneous determination of relative humidity and ammonia in air employing an optical fibre sensor and artificial neural network," (2001), 74, pp. 60–68.
14. E. C. Dickey, O. K. Varghese, K. G. Ong, D. Gong, M. Paulose, and C. A. Grimes, "Room Temperature Ammonia and Humidity Sensing Using Highly Ordered Nanoporous Alumina Films," Sensors **2**, 91–110 (2002).
15. M. L. Gorodetsky, A. A. Savchenkov, and V. S. Ilchenko, "Ultimate Q of optical microsphere resonators," Opt. Lett. **21**, 453 (1996).
16. A. K. Mallik, D. Liu, V. Kavungal, Q. Wu, G. Farrell, and Y. Semenova, "Agarose coated spherical micro resonator for humidity measurements," Opt. Express **24**, 21216–21227 (2016).
17. A. K. Mallik, G. Farrell, D. Liu, V. Kavungal, Q. Wu, and Y. Semenova, "Silica Gel Coated Spherical Micro resonator for Ultra-High Sensitivity Detection of Ammonia Gas Concentration in Air," Sci. Rep. **8**, 1620 (2018).
18. D. Liu, W. Han, A. K. Mallik, J. Yuan, C. Yu, G. Farrell, Y. Semenova, and Q. Wu, "High sensitivity sol-gel silica coated optical fiber sensor for detection of ammonia in water," Opt. Express **24**, 24179 (2016).
19. C. Malins, A. Doyle, B. D. MacCraith, F. Kvasnik, M. Landl, P. Simon, L. Kalvoda, R. Lukas, K. Pufler, and I. Babusík, "Personal ammonia sensor for industrial environments," J. Environ. Monit. **1**, 417–422 (1999).
20. B. Timmer, W. Olthuis, and A. Van Den Berg, "Ammonia sensors and their applications - A review," (2005).
21. F. X. Wei, X. F. Hu, B. Xu, M. H. Zhang, S. Y. Li, Q. Y. Sun, and P. Lin, "Ammonia concentration and relative humidity in poultry houses affect the immune response of broilers," Genet. Mol. Res. **14**, 3160–3169 (2015).
22. A. Buckley and M. Greenblatt, "The sol-gel preparation of silica gels," J. Chem. education **71**, 599–602 (1994).
23. G. Brambilla, V. Finazzi, and D. J. Richardson, "Ultra-low-loss optical fiber nanotapers," Opt. Express **12**, 2258 (2004).
24. I. M. White and X. Fan, "On the performance quantification of resonant refractive index sensors," Opt. Express **16**, 1020 (2008).